JOURNAL OF MAGNETIC RESONANCE **129,** 161–164 (1997)
ARTICLE NO. MN971257

Diffusion Measurement in Phantoms and Tissues Using SLIM Localization

Yihong Yang,[1] Su Xu,[1] M. Joan Dawson, and Paul C. Lauterbur

Biomedical Magnetic Resonance Laboratory, University of Illinois at Urbana–Champaign, Urbana, Illinois 60801

Received February 17, 1997; revised August 12, 1997

A new approach to efficient localized diffusion measurements has been developed and evaluated on phantoms and isolated tissues. The combination of a diffusion-sensitive pulse sequence with SLIM (spectral localization by imaging) makes efficient and accurate localized water and metabolite diffusion measurements possible with a substantial improvement in spatial or time resolution compared to standard methods. Phantom experiments showed that diffusion of substances present in relatively low concentration within small compartments can be measured accurately by this method, suggesting potential applications for diffusion measurements of metabolites *in vivo.* **Experiments on excised rat uterine horns demonstrated the ability of this method to measure localized diffusion of water within irregularly shaped regions of biological samples. Accurate diffusion measurements were achieved in the localized regions with acquisition times less than would have been required by standard diffusion imaging methods.** © 1997 Academic Press

Diffusion-weighted imaging (*1–4*), which has proved useful in a number of neurological (*5–8*) and other (*9*) applications, could benefit from improvements of spatial and/or temporal resolution. Similarly, measurement of metabolite diffusion in tissues has been conducted predominantly by spectroscopic techniques (*10–13*) but remains challenging due to the typically low concentration of tissue metabolites. We show here that the combination of a diffusion-sensitive pulse sequence with SLIM (spectral localization by imaging) localization makes efficient water and metabolite diffusion imaging possible, with a substantial improvement in spatial or time resolution. This method was validated by phantom experiments on metabolite diffusion and was applied to measurement of water diffusion in rat uteri.

SLIM is a non-Fourier-based localized spectroscopy method (*14, 15*) which enhances effective resolution by employing *a priori* information, in this case the high-resolution proton image, to constrain signals in the resulting spectroscopic image reconstruction. The accuracy of SLIM, including SLIM studies of inhomogeneous compartments, has been verified using simulations and experiments on phantoms (*15, 16*), as well as in ^{31}P spectroscopy studies of human brain (*17*) and excised uterus (*18*). ^{1}H SLIM has been combined with quantum coherence transfer methods for imaging lactate in muscle and brain (*19, 20*). The pulse sequence used in the present experiments for localized diffusion measurement of water or metabolites is shown in Fig. 1. For the metabolite diffusion study, this was combined with a water suppression scheme consisting of frequency-selective RF pulses and crusher gradients. Phase-encoded spectroscopic signals were combined with a high-resolution water image to achieve spatial localization. A series of localized spectra with varied diffusion weightings was obtained by SLIM analysis, and the diffusion coefficients in each of the localized regions were calculated from the intensities of the spectra. The sequence can easily be modified for measurements in a 2D slice by replacing the hard RF pulses with slice-selective pulses along with slice-selective gradients, and eliminating the phase-encoding gradients in the slice direction.

Both phantom and biological experiments were performed on a Varian VXR-500S spectrometer equipped with a Doty microimaging probe. The phantom was composed of 100 mM creatine and 100 mM lactic acid (both dissolved in 99.9% D_2O) in two separate capillaries (1-mm inner diameter) inserted parallel to the long axis of a tube (5-mm inner diameter) filled with 99.9% D_2O (Fig. 2a). The total absolute amount of each metabolite was 785 μmol. A proton spectrum of the entire phantom obtained with a single-pulse sequence is shown in Fig. 2b, and peaks in the spectrum are identified for the two components.

The diffusion gradient strength varied from 0 to 16.8 G/cm with six levels. The gradient pulse duration (δ) was 7 ms and the gradient separation (Δ) was 14 ms. For each diffusion gradient strength, phase-encoding gradients (4×4) were applied along orthogonal directions in the transverse plane, with a step size of 0.114 G/cm and a duration of 4.1 ms in both directions. Echo time (TE) and repetition time

[1] Current address: National Institutes of Health, Laboratory of Diagnostic Radiology Research, OIR, Building 10, Room B1N-256, Bethesda, MD 20892.

1090-7807/97 $25.00
Copyright © 1997 by Academic Press
All rights of reproduction in any form reserved.

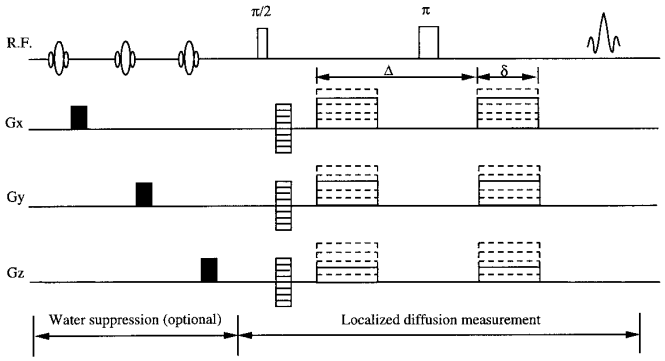

FIG. 1. Pulse sequence for localized diffusion measurement. Localized spectra in regions of interest were obtained from the phase-encoded signals combined with an anatomic image. The spectra were weighted by the diffusion-sensitizing gradients, and diffusion coefficients in the local regions were calculated by fitting the intensities of the diffusion-weighted spectra.

(TR) were 30 and 1000 ms, respectively. The structure of the phantom was determined by a spin-echo proton image (128×128) from the HDO in the phantom, with the transmit frequency at the proton resonance frequency of HDO. The image was segmented into three compartments, the capillary containing creatine, the capillary containing lactic acid, and the tube outside the two capillaries.

Data were processed off-line on a SUN SPARC workstation (Sun Microsystems, Mountain View, CA) using the publicly available signal processing package VIEWIT (*21*). For each diffusion gradient strength, the diffusion-weighted spectra from the creatine capillary, lactic acid capillary, and the outer compartment were obtained from the phase-encoded spectroscopic signals and the segmented image by SLIM analysis. The localized spectra of the three compartments at each diffusion gradient strength are shown in Fig. 3. Magnitude spectra were used for calculating diffusion coefficients, in order to avoid introducing errors associated with complicated phase correction. Spectra from these compartments were well separated, with negligible contamination (less than 2.0% signal leakage). For comparison, contamination of the creatine compartment by signal from lactate was 12.4%, and contamination of the lactate compartment by creatine was 14.3% in the CSI (chemical shift imaging) analysis of these same data. Diffusion coefficients of the creatine and lactic acid were calculated by least-squares fitting of the signal intensities of their methyl groups. At 23.2°C, the diffusion coefficients of the lactic acid and creatine were measured to be 0.49 ± 0.04 and $0.69 \pm 0.05 \times 10^{-3}$ mm^2/s, respectively. For comparison, their diffusion coefficients were measured individually without spatial localization at the same temperature. The individually measured diffusion coefficients of lactic acid and creatine were 0.48 ± 0.03 and $0.68 \pm 0.04 \times 10^{-3}$ mm^2/s, respectively.

A SLIM-localized water diffusion measurement was performed on biological samples. Rat uterine horns were selected because they are composed of distinct tissue layers (longitudinal and circular muscles, and endometrium), and the water diffusion in these tissues has been measured (*22*). In the rat uterine horn studies, the whole rat uterus was removed after sacrifice of the animal and a single 3- to 4-cm segment of uterine horn was inserted immediately into a tube (4-mm inner diameter). Animal and tissue handling

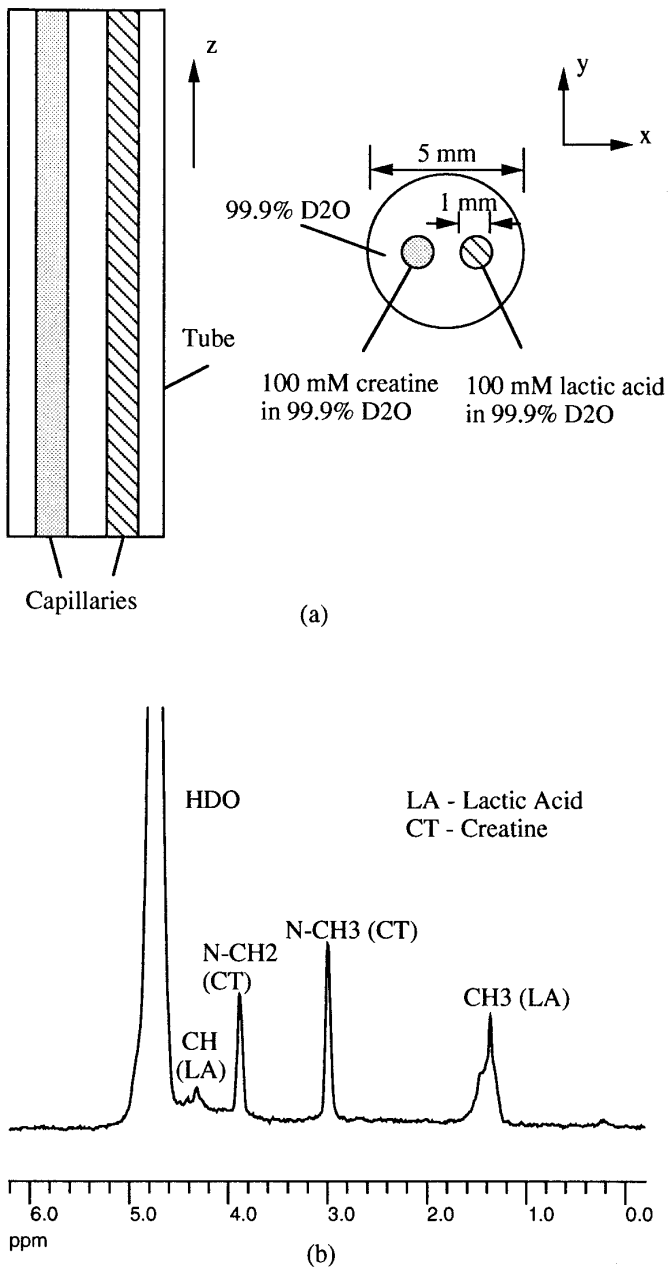

FIG. 2. (a) Schematic diagram of the phantom used in the experiments. Two separate capillaries containing 100 mM creatine and 100 mM lactic acid (both dissolved in 99.9% D_2O) were inserted into a tube filled with 99.9% D_2O. (b) Proton spectrum of the entire phantom obtained with a single-pulse sequence. Peaks in the spectrum are identified for the two compounds.

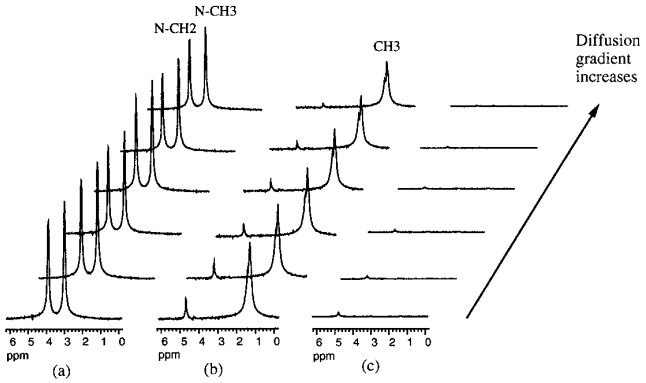

FIG. 3. The localized proton spectra from the phantom obtained by SLIM analysis using a 4 × 4 phase-encoding data set at each diffusion gradient strength. (a) Spectra from the capillary containing creatine in 99.9% D_2O, (b) spectra from the capillary containing lactic acid in 99.9% D_2O, and (c) spectra from the outer compartment (99.9% D_2O only).

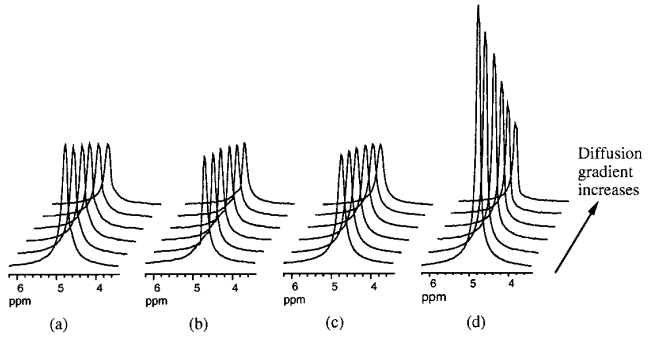

FIG. 5. The localized proton spectra of (a) longitudinal muscle, (b) circular muscle, (c) endometrium, and (d) lumen fluid, from a transverse slice of a rat uterine horn, obtained by SLIM analysis using an 8 × 8 phase-encoding data set for each gradient strength.

was as previously described (*22*), and was approved by the Laboratory Animal Care Advisory Committee of the University of Illinois at Urbana–Champaign. A 2D version of the localized diffusion sequence was used to measure water diffusion coefficients in a 2-mm transverse slice of the endometrium and the longitudinal and circular muscle layers. Diffusion-sensitizing gradient strength, duration, and steps were the same as in the phantom experiment, with the direction of the gradients along the long axis of the uterine horn (parallel to the longitudinal muscle and perpendicular to the circular muscle fibers). Phase encodings (8 × 8) were applied along orthogonal directions in the transverse slice. TE and TR were 32 and 1000 ms, respectively. A spin-echo image and a diffusion map (diffusion along the uterine horn, D_z) of the 2-mm transverse slice are shown in Figs. 4a and 4b. Contrasts among longitudinal and circular muscle, endometrium, and lumen fluid are clearly shown in the diffusion map. A ''mask'' composed of four segmented compartments corresponding to the four regions (Fig. 4c) was used for SLIM analysis.

Localized proton spectra of the four compartments for each diffusion gradient strength are shown in Fig. 5. The water diffusion coefficients of the longitudinal and circular muscle, endometrium, and fluid in lumen at 23.2°C were measured to be 1.28 ± 0.10, 0.83 ± 0.06, 0.95 ± 0.07, and 2.04 ± 0.09 × 10^{-3} mm^2/s, respectively. The significant differences in diffusion coefficients for the circular and longitudinal muscle is due to diffusion anisotropy; the diffusion gradients were applied parallel to the longitudinal muscle fibers and perpendicular to the circular muscle fibers (*22*). These diffusion coefficients agreed well with the results obtained by conventional diffusion imaging in the same regions and directions (1.23 ± 0.09, 0.81 ± 0.08, 0.97 ± 0.08, and 2.05 ± 0.10 × 10^{-3} mm^2/s in the longitudinal and circular

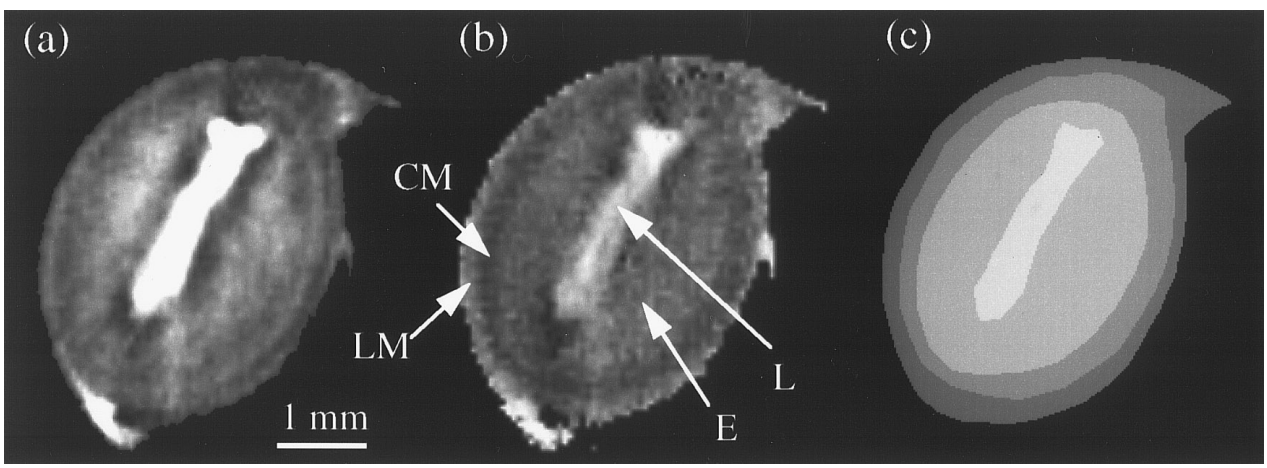

FIG. 4. (a) A spin-echo image (TE/TR = 20/3000 ms), and (b) a diffusion map (D_z) of a transverse slice of a rat uterine horn. Image contrasts among longitudinal muscle (LM), circular muscle (CM), endometrium (E), and lumen (L) are clearly shown in the diffusion map. The diffusion-weighted images used to obtain the diffusion map were acquired with 128 phase-encoding steps, 6 diffusion gradient steps, and a TR of 3 s. (c) A mask composed of four segmented compartments corresponding to the four structures.

muscle, endometrium, and fluid in lumen, respectively). For the conventional diffusion imaging experiment, a longer TR (3 s) was needed to obtain sufficient signal-to-noise ratio to determine the diffusion coefficients with the same precision as in the SLIM experiment. The acquisition time for the SLIM diffusion experiment was 384 s (8×8 phase-encoding steps, 6 diffusion gradient steps, and TR = 1 s), compared to 2304 s for the conventional diffusion imaging.

We have demonstrated efficient and accurate localized diffusion measurements of water and metabolites in phantoms and tissues using SLIM localization. The phantom experiments showed that diffusion of substances present in relatively low concentrations within small compartments can be measured accurately by this method, indicating potential applications for diffusion measurement of metabolites *in vivo*. The high sensitivity was achieved by collecting signals contributed from the entire spin population in each localized region. Experiments on rat uterine horns demonstrated the ability of this method to measure localized diffusion of water within slices from irregularly shaped regions on biological samples, and accurate diffusion measurement was achieved in the localized regions with reduced acquisition time.

The SLIM diffusion method presented here is useful for regions of tissue that have visible boundaries. Those boundaries may reflect weighting by proton density, chemical composition (fat vs water), T1, T2, apparent diffusion coefficients, etc. For example, a diffusion-weighted image may reveal the extent of a region in acute stroke, whose boundaries can then be useful in a SLIM analysis for determining, with great accuracy and precision, the average diffusion coefficient and its change with time. When boundary information is insufficient for SLIM analysis, alternative methods would be more appropriate. These include GSLIM (generalized SLIM, Ref. *15*), which can reveal compartmental inhomogeneities and compensate for them (*16*). SLIM and GSLIM analysis can be used with EPI and other fast scan techniques, resulting in a decrease in acquisition time which is similar in extent to that for Fourier-based imaging.

ACKNOWLEDGMENTS

This work was supported by NIH Grants PHS 5P41 RR05964, 1S10RR06243, and PHS 1 R01 CA51430.

REFERENCES

1. E. G. Wesby, M. E. Moseley, and R. L. Ehman, *Invest. Radiol.* **19,** 491–498 (1984).
2. K.-D. Merboldt, W. Hanicke, and J. Frahm, *J. Magn. Reson.* **64,** 479–486 (1985).
3. D. G. Taylor and M. C. Bushell, *Phys. Med. Biol.* **30,** 345–349 (1985).
4. D. Le Bihan, E. Breton, D. Lallemand, *et al., Radiology* **161,** 401–407 (1986).
5. M. E. Moseley, Y. Cohen, J. Mintorovitch, L. Chileuitt, H. Shimizu, J., Kucharczyk, M. F. Wendland, and P. R. Weinstein, *Magn. Reson. Med.* **14,** 330–346 (1993).
6. S. Warach, D. Chien, W. Li, M. Ronthal, and R. R. Edelman, *Neurology* **42,** 1717–1723 (1992).
7. M. E. Moseley, Y. Cohen, J. Kucharczyk, J. Mintorovitch, H. S. Asgari, M. F. Wendland, J. Tsuruda, and D. Norman, *Radiology* **176,** 439–449 (1990).
8. M. A. Rutherford, F. M. Cowan, A. Y. Manzur, L. M. S. Dubowitz, J. M. Pennock, J. V. Hajnal, I. R. Young, and G. M. Bydder, *J. Comput. Assist. Tomogr.* **15,** 188–198 (1991).
9. D. Le Bihan, *Magn. Reson. Q.* **7,** 1–30 (1991).
10. K. Yoshizaki, Y. Seo, H. Nishikawa, and T. Moromoto, *Biophys. J.* **38,** 209–211 (1982).
11. C. T. W. Moonen, P. C. M. Van Zijl, D. Le Bihan, and D. DesPres, *Magn. Reson. Med.* **13,** 467–477 (1990).
12. K.-D. Merboldt, D. Horstermann, W. Hanicke, H. Bruhn, and J. Frahm, *Magn. Reson. Med.* **29,** 125–129 (1993).
13. S. Posse, C. A. Cuenod, and D. Le Bihan, *Radiology* **188,** 719–725 (1993).
14. X. Hu, D. N. Levin, P. C. Lauterbur, and T. Spraggins, *Magn. Reson. Med.* **8,** 314–322 (1988).
15. Z.-P. Liang and P. C. Lauterbur, *IEEE Trans. Med. Imaging* **10,** 132–137 (1991).
16. Z.-P. Liang and P. C. Lauterbur, *J. Magn. Reson. B* **102,** 54–60 (1993).
17. Y. Yang, Magnetic resonance diffusion imaging and spectral localization: New methods and their quantitative applications, Ph.D. thesis, University of Illinois at Urbana–Champaign (1995).
18. S. Xu, Y. Yang, C. D. Gregory, J. C. Vary, Z.-P. Liang, and M. J. Dawson, *Magn. Reson. Med.* **37,** 736–743 (1997).
19. J. A. Kmiecik, C. D., Gregory, Z.-P. Liang, D. E. Hrad, P. C. Lauterbur, and M. J. Dawson, *Magn. Reson. Med.* **37,** 840–850 (1997).
20. J. A. Kmiecik, C. D. Gregory, Z.-P. Liang, P. C. Lauterbur, and M. J. Dawson, *in* ''Proceedings, ISMRM, 5th Annual Meeting, Vancouver, Canada,'' p. 602 (1997).
21. C. Potter and P. J. Moran, *in* ''Annual SPIE Conference on Biomedical Imaging Processing and Three-Dimensional Microscopy,'' pp. 767–773 (1992).
22. Y. Yang, S. Xu, and M. J. Dawson, *Magn. Reson. Med.* **33,** 732–735 (1995).